

Supplementary Information Appendix

A Late Pleistocene coastal ecosystem in French Guiana was hyperdiverse relative to today

Pierre-Olivier Antoine, Linde Wieringa, Sylvain Adnet, Orangel Aguilera, Stéphanie Bodin, Stephen Cairns, Carlos A. Conejeros-Vargas, Jean-Jacques Cornée, Žilvinas Ežerinskis, Jan Fietzke, Natacha O. Gribenski, Sandrine Grouard, Austin Hendy, Carina Hoorn, Renaud Joannes-Boyau, Martin R. Langer, Javier Luque, Laurent Marivaux, Pierre Moissette, Kees Nooren, Frédéric Quillévéré, Justina Šapolaitė, Matteo Sciumbata, Pierre G. Valla, P., Nina H. Witteveen, Alexandre Casanova, Simon Clavier, Philibert Bidgrain, Marjorie Gallay, Mathieu Rhoné & Arnauld Heuret

1. Material

The fossil material belongs to the collection of the Université de Guyane, France. Whenever possible, i.e., if large numbers of specimens are available for a given species, a part of the collection is further stored in the collections of the Université de Montpellier, France.

1.1. Sampling localities

Table S1: Sampling localities in Pleistocene–Holocene sections around the ELA4 Ariane 6 launcher pad, Kourou, French Guiana. ASL, above sea-level.

<i>Name</i>	<i>Latitude (N)</i>	<i>Longitude (W)</i>	<i>Height (top)</i>	<i>Sampling date</i>	<i>Sampled for</i>
KOU-AR6-01	5°15.878'	52°47.650'	6 m ASL	February 14, 2019	Macrofossils
KOU-AR6-02	5°15.957'	52°47.496'	6 m ASL	February 14, 2019	Macrofossils
KOU-AR6-03	5°15.893'	52°47.455'	6 m ASL	April 8, 2019	Macrofossils, Microfossils, Pollen, U-series dating
KOU-AR6-04	5°15.739'	52°47.404'	9 m ASL	April 9, 2019	Charcoal, ¹⁴ C dating
KOU-AR6-05	5°15.901'	52°47.463'	6 m ASL	April 11, 2019	Macrofossils, Microfossils
KOU-AR6-06	5°16.135'	52°47.324'	4 m ASL	October 7, 2021	Macrofossils, Microfossils, Pollen- phytoliths, U-Th dating, OSL dating

KOU-AR6-01 locality



Fig. S1. Trench KOU-AR6-01, with giant exhaust-aimed and gantry infrastructures for Ariane 6 in the background (top left and right, respectively). Water fills the bottom of the stratigraphic sequence, thus covering the basal oyster-rich conglomerate and grey clays, being sampled by the excavator bucket.
Photograph by A.H.

Nature: trench

Investigated in: February 14, 2019

Access: excavated and filled up immediately

Amount of sediment sampled: unknown (>100 kg), in basal oyster-rich conglomerates and grey clays

Handpicking: yes

Screenwashing: yes

KOU-AR6-02 locality



Fig. S2. Trench KOU-AR6-02. The complete sequence is visible. Photograph by A.H.

Nature: trench

Investigated in: February 14, 2019

Access: excavated and filled up immediately

Amount of sediment sampled: unknown (>100 kg), in basal oyster-rich conglomerates and grey clays

Handpicking: yes

Screenwashing: yes

KOU-AR6-03 locality



Fig. S3. Trench KOU-AR6-03. The complete sequence is visible, starting from the top of pink saprolites (bottom) overlaid by basal oyster-rich conglomerate and grey clays. Photograph by P.-O.A.

Nature: trench

Investigated in: April 8, 2019

Access: excavated and filled up immediately

Amount of sediment sampled: 320 kg in basal conglomerates and grey clays (Base); 30 kg in kaki conglomerate and clays (Top)

Handpicking: yes

Screenwashing: yes

Sampled for: Macrofossils, Microfossils, Pollen, U-Th dating

KOU-AR6-04 locality



Fig. S4. Ditch KOU-AR6-04 (detail). Only the topping sequence, of continental origin, is accessible. Note the presence of in-situ charcoals. Photograph by P.-O.A.

Nature: ditch
Investigated in: April 9, 2019
Access: accessible
Amount of sediment sampled: N/A
Handpicking: yes (tree stumps and loose charcoals)
Screenwashing: No
Sampled for: Charcoal, ^{14}C dating

KOU-AR6-05 locality



Fig. S5. Trench KOU-AR6-05, with the Ariane 6 rocket gantry in the background (left). The complete stratigraphic sequence is visible, starting by the basal oyster-rich conglomerate and grey clays.
Photograph by P.-O.A.

Nature: trench

Investigated in: April 11, 2019

Access: excavated and filled up immediately

Amount of sediment sampled: 150 kg in kaki conglomerate and clays (Top)

Handpicking: yes

Screenwashing: yes

Sampled for: Macrofossils, Microfossils

KOU-AR6-06 locality



Fig. S6. Trench KOU-AR6-06. To the left, sampling for OSL-dating (OSL-1). On the right side of the trench, sampling for pollen and phytoliths (KOU-AR6-06 PN-10 to PN-15). At top right, macrofossil and microfossil sampling for oyster-rich deposits extracted through the excavator bucket, lower in the marine sequence (not visible). Photograph by L.M.

Nature: trench

Investigated in: October 7, 2021

Access: excavated and filled up immediately

Amount of sediment sampled: 255 kg in basal conglomerates and grey-kaki clays (Base); 15 kg in kaki clays (Top)

Handpicking: yes

Screenwashing: yes

Sampled for: Macrofossils, Microfossils, Pollen, U-Th dating, OSL dating, ¹⁴C dating

2. Methods

2.1. Fossil preparation, extraction, and analysis

2.1.1. Macrofossil and microfossil sampling, screen-washing, and subsequent study

All the fossil remains described here were found in-situ by our consortium in 2018, 2019, and 2021. Some macro-remains (e.g., oysters, wood chunks, and large selachian teeth) were hand-picked directly in the field and properly located/labelled. All other fossil specimens were collected by screening-washing of clays, silts, and conglomerates, with a 2 mm, 1 mm, and/or 0.7 mm mesh. Smaller sieves were used for microvertebrates (0.4 mm) and foraminifers (150 and 63 μ m). Foraminifers were only retrieved within connected valves of large bivalves. Their absence in all other marine samples is most likely due to post-burial dissolution of their tests, which likely further resulted in a lower taxonomic diversity recorded. No acid etching has been performed, in order to preserve delicate calcified shells, either visible or invisible to the unaided eye.

The fossil specimens were curated in separate ziplocks with adequate labels (location/date/sampling locality/sampling level/subsample, etc.), and subsequently sent to colleagues with the best expertise on the taxonomic group concerned. Over 1,000 kg of sediment have been screen-washed in total.

2.1.2. Charcoal identification

Charcoals were manually broken according to the three planes of wood – transverse, radial longitudinal and tangential longitudinal – and observed under a reflected light microscope equipped with dark and bright fields at x10, x20 and x50 magnifications. Charcoal identification was performed after comparison with the wood charcoals from the reference collection from French Guiana located at the Institut des Sciences de l'Evolution de Montpellier (1) and with the help of identification tools (2–4).

2.1.3. Phytolith extraction and analysis

After adding 56.000 microspheres, the phytolith samples were boiled four times in 33% H₂O₂ and treated with 10% HCl and KMnO₄ to remove organic matter. After decanting, phytoliths were extracted using Bromoform (specific gravity 2.3) (5) and mounted on microscope slides using Permount. Phytoliths were counted using the Zeiss Axioscope. For samples PN15A and PN15B, a sum of 400 phytoliths were counted at 630X magnification. For samples PN9-PN14, the concentration of phytoliths was too low to obtain a full count. Instead, the slides were scanned at 400X magnification. Phytolith morphotypes were classified according to literature (6–8).

2.1.4. Pollen extraction and analysis

**KOU-AR6-03 trench*

Nine samples of 1 and 2 cm³ from nine different depth intervals (PN0–PN8, see Fig. S11) were processed for pollen analysis. Only PN6 yielded a decent pollen recovery, with not enough grains for being counted, though.

**KOU-AR6-06 trench*

Eleven subsamples of 1 and 2 cm³ from seven different depth intervals (PN9–PN15, see Fig. S11) were processed for pollen and phytolith analysis. Pollen samples were processed conform standard palynological extraction procedures (9). *Lycopodium* tablets were added to allow the calculation of pollen concentration. A minimum of 300 pollen grains was counted using a 400x magnification light microscope. Fern spores other than *Acrostichum*, and Cyperaceae were not included in the pollen sum. Results are presented as a percentage of the pollen sum. Samples PN10 – PN14 were completely devoid of pollen. Therefore, only samples from two depth intervals (PN9 and PN15) could be counted.

2.2. Dating methods

2.4.1. Optically-Stimulated Luminescence (OSL)

Samples for OSL dating were collected with metal tubes pounded into fresh sediment, and have been prepared at the Institute of Geological Sciences (Univ, Bern) following the protocol described in Lowick et al. (10). Under subdued laboratory illumination, samples were treated with HCl (32%) and H₂O₂ (30%) to remove carbonates and organic components, respectively. Quartz fine-sand fractions were isolated following sieving (63-100µm) and density separation using LST Fastfloat heavy liquid at 2.70 g cm⁻³. The fine-grained quartz was etched in 40% hydrofluoric acid for 1 h (to remove any feldspar contamination), rinsed and then immersed in 32% hydrochloric acid for 1 h to remove fluorides. Fine quartz grains were settled on 10-mm diameter stainless steel discs using silicon spray (4-mm diameter mask).

All luminescence measurements were carried out using TL/OSLDA-20 Risø readers, equipped with a calibrated ⁹⁰Sr/⁹⁰Y beta source (Institute of Geological Sciences, Univ. Bern). Luminescence signals were detected using an EMI 9235QA photomultiplier tube, with stimulation at 90% power using blue LEDs at 125°C, and with the signal detected through 7.5-mm of Hoya U-340 transmission filter.

All equivalent dose (De) measurements were performed using a modified (post-IRSL) SAR protocol (11, 12). A preheat of 200°C for 10 s was applied to ensure that the protocol was able to recover a regenerated dose to within 10% of unity (and in addition this protocol provided low/negligible residuals). De values were calculated using the first 0.8 s of the OSL signal, using an early background correction (first 10s after OSL signal integral) and an exponential fitting for constructing the dose-response curves. All aliquots met the following criteria: (1) recycling ratios within 10% of unity, (2) recuperation values below 10%, and (3) IR-depletion ratio below 15% (13).

About 100 g of bulk sediment material was collected from the surrounding of each sample to determine the environmental dose rate. The material was desiccated at 60 °C to enable water content quantification. U, Th and K activities were measured using high-resolution gamma spectrometry [Department of Chemistry and Biochemistry, Univ. Bern (14)] and were employed, together with the measured water content, as inputs for final dose rate determination through the Dose Rate and Age Calculator [DRAC (15)]. We used the Luminescence R package (16) to quantify the Central Age Model (CAM) (17) for both samples.

2.4.2. U-Th dating (conventional solution)

Conventional solution U/Th dating of coral fragments from KOU-AR6-06 (base) has been carried out using a Thermo Neptune plus at GEOMAR Helmholtz Center for Ocean Research Kiel, Germany. The procedures (chemical preparation and separation, analyses) followed the approach described by Fietzke et al. (18). This included the use of a Th229/U233/U236 mix spike, added after sample dissolution prior to the chemical separation of the Th and U from the sample matrix. The results of this analysis are summarized in Table S4.

For the correction of non-radiogenic Th230 a detrital Th230/Th232 activity ratio of 0.6 ± 0.2 has been applied. The back-calculated initial U234/U238 activity ratio is slightly higher than the typical open-ocean ratio, which is taken as indication of a small potential loss of uranium from the sample. Considering this, the calculated age should be interpreted as a maximum value.

2.4.3. U-Th dating (laser ablation)

Twelve *Astrangia rathbuni* corals were sampled at the bottom of the KOU-AR6-03 trench, to obtain uranium-series ages. Uranium-series measurements were undertaken by laser ablation Multi Collector-Inductively Coupled Plasma Mass Spectrometer (MC-ICPMS) at the Geoarchaeology and Archaeometry Research Group (GARG) Biomics facility, Southern Cross University. Laser ablation was performed with a New Wave Research 213 nm laser, equipped with a TV2 cell. Thorium (^{230}Th , ^{232}Th) and uranium (^{234}U , ^{235}U , ^{238}U) isotopes were measured on a Thermo Neptune XT MC-ICPMS mounted with jet sample and x-skimmer cones. All five isotopes were collected in static mode, with both ^{234}U and ^{230}Th collected in the ion counter and CDD respectively. Helium flow rate and ICP-MS parameters were tuned with NIST610 element standard to derive a $^{232}\text{Th}/^{238}\text{U}$ ratio greater than 0.80. Tuning was achieved with a fluence of 10.3 J/cm², pulse rate of 20 Hz, spot size of 110 μm and scan speed of 5 $\mu\text{m}/\text{s}$, yielding 1.91V of ^{238}U and 1.57V of ^{232}Th on NIST610.

Because of their size, samples had to be mounted in resin and then polished to 5micron smoothness. Each sample was then ablated using rasters of 5min each (twice $\sim 750 \mu\text{m}$ long). Before and after each sample, NIST612, MK10 and MK16 (19) standards were measured. $^{234}\text{U}/^{238}\text{U}$ and $^{230}\text{Th}/^{238}\text{U}$ isotopic ratios were corrected for elemental fractionation and Faraday cup/SEM yield by comparison with MK10 coral for which ratios were previously characterized internally by solution analysis. Detrital-corrected ^{230}Th -U ages were calculated for each analysis using IsoPlotR (20) with an assumed detrital ($^{230}\text{Th}/^{232}\text{Th}$) activity ratio of 0.8 ± 0.8 . Concentrations of U and Th were determined using NIST612 glass as a calibration standard. Background subtraction, concentration quantification and ratio corrections were performed using Lolite™ software (21). The corrected ($^{234}\text{U}/^{238}\text{U}$) and ($^{230}\text{Th}/^{238}\text{U}$) isotope ratios for the secondary standard (MK16 coral) within error of the value determined by solution analysis.

2.4.4. Radiocarbon analysis

Charcoals were identified before being sent for dating to ensure they belong to different taxa and hence from different individuals (22). Furthermore, whenever possible, charcoals from twigs or short-lived taxa were selected for dating to avoid the old wood effect (23).

Charcoal samples were dated at the Accelerator Mass Spectrometry Laboratory, Center for Physical Sciences and Technology in Vilnius (Vilnius Radiocarbon). Before radiocarbon (^{14}C) measurements, the samples had to be graphitized first. Graphitization was performed with Automated Graphitization System (AGE-3, Ionplus AG). Chemical preparation of charcoal samples was performed using the standard acid–base–acid method (24). The chemical treatment steps were as follows: 1M hydrochloric acid, 0,1M sodium hydroxide and 1M hydrochloric acid. A Single-stage Accelerator Mass Spectrometer (SSAMS, NEC, USA) was used for radiocarbon measurements. Phthalic anhydride was used for the estimation of the background of measurements (2.45×10^{-3} fM (fraction of modern carbon)). The NIST-OXII (134.06 pMC) standard was used as reference material. The $^{14}\text{C}/^{12}\text{C}$ ratio was measured with an accuracy better than 0.3%. For the isotopic fractionation correction, the ratio of ^{13}C to ^{12}C was used. All dates were calibrated by OxCal v4.4.4 (25) following the IntCal20 atmospheric curve (26).

3. Results

3.1. Age constraints

3.1.1. OSL age constraints

For OSL dating, luminescence measurements showed that almost all aliquots were close to saturation, and thus to the dating limit of the quartz OSL method. As a consequence, OSL age constraints must be taken as minimum age estimates, given that the coastal depositional environments for these sediments would a priori present any major issue of pre-depositional partial bleaching of the OSL signal. For

discussion, we estimated two OSL age constraints for samples OSL-1 and OSL-2, either considering all aliquots providing a D_e value (column 5 in Table S2) or by considering only aliquots below saturation (column 6 in Table S3). OSL results show very similar age estimates (within errors) for the two samples, and in the main text we report minimum age estimates using only aliquots below saturation.

Table S2. OSL dating results. Analytical details and measurement protocols are given in the main text. ¹A total of 24 aliquots have been measured for each sample. Some aliquots did not provide any D_e value (natural OSL signal on/above the dose-response plateau), and for aliquots with D_e values some were in saturation [$D_e > 2 * D_0$ (27)]. ²⁻³ D_e = Equivalent doses (non-corrected for residuals), CAM = Central Age Model, OD = overdispersion of D_e distribution (17). For (2), CAM D_e values and OSL ages have been estimated using all aliquots providing a D_e estimate. For (3), CAM D_e values and OSL ages have been estimated using all non-saturated aliquots.

Sample	Nb aliquots ¹ (D_e /Non-saturated)	CAM ² D_e (Gy) (OD %)	CAM ³ D_e (Gy) (OD %)	CAM OSL ² age (ka)	CAM OSL ³ age (ka)
OSL-1	6/1	225.1±14.1 (8.9)	194.9±10.5 (/)	138.3±12.6	119.7±10.2
OSL-2	8/2	233.2±24.1 (26.4)	168.9±26.5 (21.1)	144.4±17.9	104.6±17.9

Table S3. Details of dose-rate calculations for OSL dating.

¹Radionuclide concentrations were quantified on bulk samples using high-resolution gamma spectrometry (Department of Chemistry and Biochemistry, Univ. Bern).

²Dose rate calculations were performed with DRAC (15), assuming water content of 25±10% and bulk sample density of 2.3±0.3 g cm⁻³.

Sample	Radionuclide concentration ¹			Grainsize (μ m)	Depth below surface (m)	Total dose rate ² (Gy ka ⁻¹)
	U (ppm)	Th (ppm)	K (%)			
OSL-1	2.03±0.11	5.93±0.30	0.99±0.05	63-100	2.1±0.1	1.628±0.11
OSL-2	1.79±0.18	6.13±0.31	1.04±0.05	63-100	3.0±0.1	1.615±0.11

3.1.2. U-Th ages

Table S4. Results of conventional solution MC-ICP-MS U-Th dating of the coral *Astrangia rathbuni*, from KOU-AR6-06 (base).

Sample	Age ky	± ky	min-Age ky	max-Age ky	U238 ppm	± ppm	Th232 ppb	± ppb
#12 Kourou	135,8	1,1	134,7	136,9	2,7922	0,0023	343	3
Sample	Th230 ppt	± ppt	Th230/Th232 dpm/dpm	± dpm/dpm	U238/Th232 dpm/dpm	± dpm/dpm	Th230/U238 dpm/dpm	± dpm/dpm
#12 Kourou	38,210	0,049	20,83	0,16	25,23	0,20	0,82541	0,00126
Sample	Th230excess/U238 dpm/dpm	± dpm/dpm	U234/U238 dpm/dpm	± dpm/dpm	U234/U238initial dpm/dpm	± dpm/dpm	238/232	232/238
#12 Kourou	0,80164	0,00188	1,108	0,00166	1,158	0,002	25,23	0,039628868

Table S5. Details of U-Th dating results on corallites of *Astrangia rathbuni* from KOU-AR6-03 (base). Ages and standard errors taken into account in the current work are bold-typed and in blue (Coral-2 and Coral_6 to Coral_12).

	U_ppm	U_ppm_Int2SE	R48	Err_R48_Int2SE	R08	Err_R08_Int2SE	Age (ka)	Err (2-SE)
Coral_1	1.04	0.38	1.13	<i>0.21</i>	<i>0.65</i>	<i>0.59</i>		
Coral_2	0.98	0.13	1.123	0.049	0.802	0.098	127.6998	25.5399
Coral_3	2.55	0.57	1.101	0.044	<i>0.928</i>	<i>0.93</i>		
Coral_4	2.62	0.71	1.059	0.038	<i>1.049</i>	<i>0.68</i>		
Coral_5	4.7	1.9	1.083	0.038	<i>1.054</i>	<i>0.087</i>	262.4702	80.9658
Coral_6	3.33	0.12	1.122	0.024	1.04	0.054	220.5032	32.4994
Coral_7	3.38	0.25	1.137	0.021	0.915	0.054	124.9245	14.3312
Coral_8	3.93	0.17	1.133	0.019	0.95	0.087	142.6015	28.5683
Coral_9	3.73	0.21	1.131	0.035	0.894	0.035	145.0988	9.3231
Coral_10	4.72	0.19	1.134	0.025	0.798	0.034	127.1405	6.9228
Coral_11	4.9	0.46	1.128	0.018	0.8	0.042	129.1681	11.4697
Coral_12	3.655	0.072	1.164	0.028	0.802	0.047	122.0262	10.3722

3.1.3. Radiocarbon datings

Table S6. Charcoal sample designation (field number / lab code) and radiocarbon ages obtained (BP and cal BP, using OxCal);

Sample designation	Lab. code	Radiocarbon age, BP	Radiocarbon age, cal BP
KOU-AR6-04-SITU-3-RUB	FTMC-HE52-3	892±30	804±55
KOU-AR6-04-SOM-40-SM	FTMC-HE52-1	1995±88	1938±120
KOU-AR6-04-LIT-2-INDET	FTMC-HE52-2	39825±288	43091±284
KOU-AR6-04-?-22-MLT	FTMC-HE52-4	44717±478	47053±572

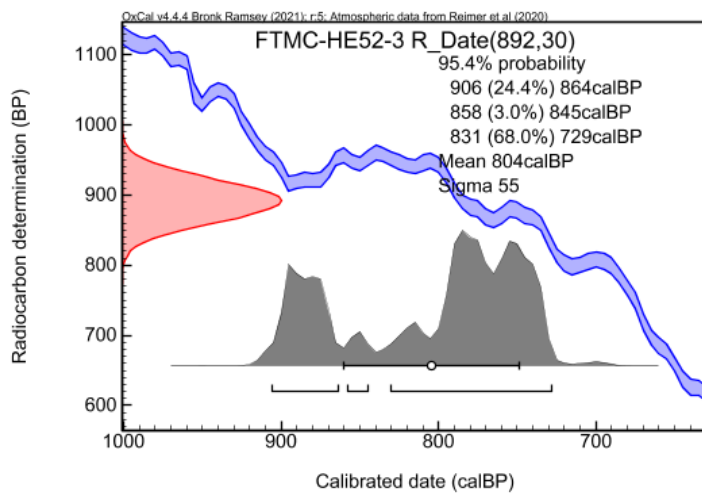


Fig. S7. Calibrated radiocarbon date before present obtained for the uppermost charcoal sample (KOU-AR6-04-SITU-3-RUB), Unit C, Top at KOU-AR6-04, through OxCal v 4.4.4 [online version (25)].

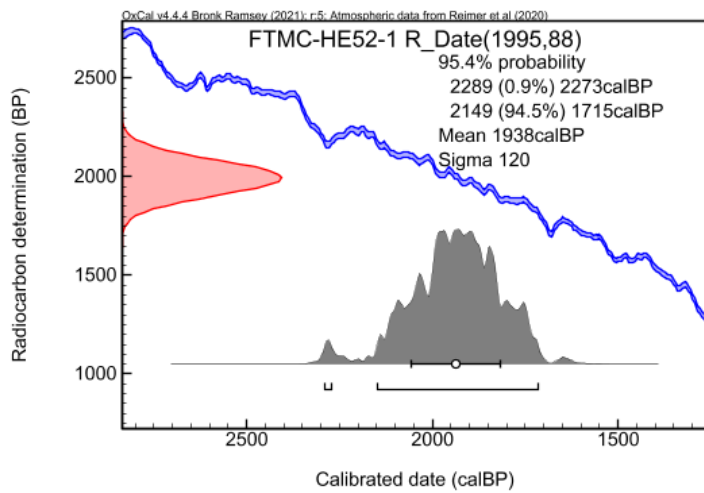


Fig. S8. Calibrated radiocarbon date before present obtained for the second uppermost charcoal sample (KOU-AR6-04-SOM-40-SM), Unit C, Top at KOU-AR6-04, through OxCal v 4.4.4 [online version (25)].

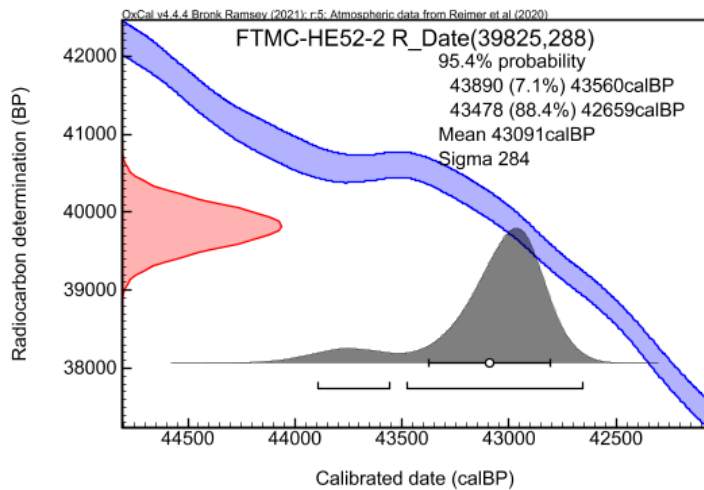


Fig. S9. Calibrated radiocarbon date before present obtained for the second lowermost charcoal sample (KOU-AR6-04-LIT-2-INDET), Unit C, Base at KOU-AR6-04, through OxCal v 4.4.4 [online version (25)].

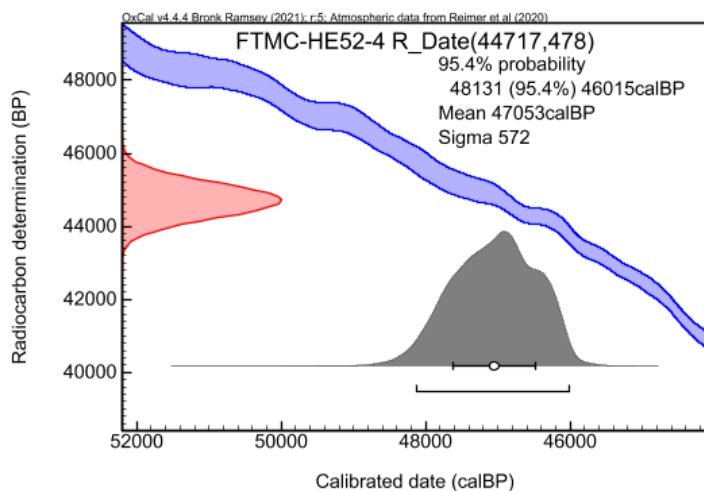


Fig. S10. Calibrated radiocarbon date before present obtained for the lowermost charcoal sample (KOU-AR6-04-?-22-MLT), Unit C, Base at KOU-AR6-04, through OxCal v 4.4.4 [online version (25)].

3.2. Stratigraphic sections

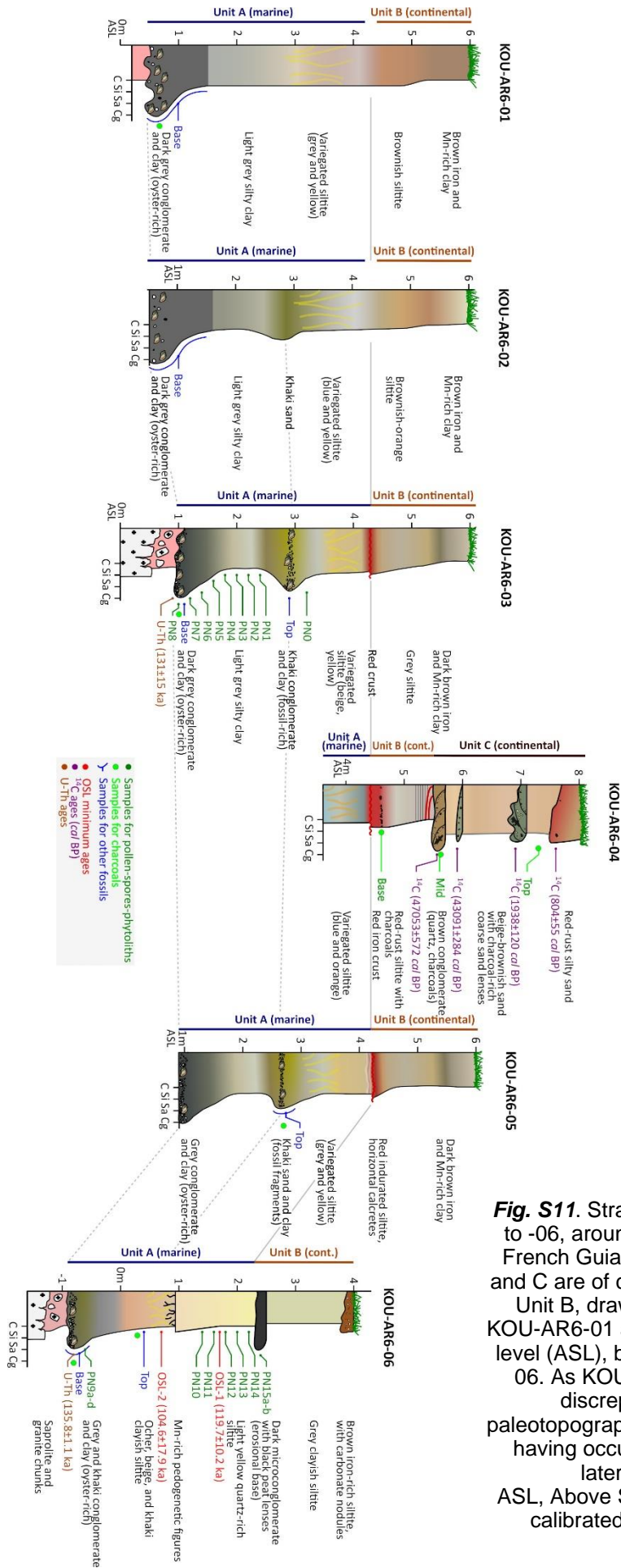


Fig. S11. Stratigraphic sections of trenches KOU-AR6-01 to -06, around the Kourou ELA4 launcher pad, Kourou, French Guiana. Unit A is of marine origin, while Units B and C are of continental origin (cont.). The baseline of the Unit B, drawn in grey, is horizontal between sections KOU-AR6-01 and -05, at 4.2–4.5 m above the recent sea-level (ASL), but it is dropping to 2.4 m ASL at KOU-AR6-06. As KOU-AR6-06 was located more seaward, this discrepancy is interpreted as resulting from paleotopography instead of differential vertical movements having occurred in the meantime. Dotted lines denote laterally-equivalent levels in the Unit A. ASL, Above Sea-Level; BP, Before Present; C, clay; cal, calibrated; Cg, conglomerate; Sa, sand; Si, siltite.

3.3. Taxonomic composition of Kourou ELA 4 biotic communities

3.3.1. Foraminifers

Communities formed by foraminifers (Fig. 2A–C) are mainly composed of hyaline-perforate benthic taxa, indicative for shallow intertidal mangrove and subtidal environments (11 species and seven genera) and one individual of planktonic foraminifer (*Globigerina bulloides*; Fig. 2D) (SI Appendix, Table S7). Their fine preservation state suggests low energy and preservation in-situ. The benthic assemblage comprises three species of Miliolida (*Quinqueloculina seminula*, Q. sp. 1 and Q. sp. 2) and eight species of Rotaliida, including three species of *Ammonia*, *Eponides repandus*, and very small foraminifer species (*Nonion subburgidum*, *Elphidium magellanicum*, *Cerebrina claricerviculata*, and *Fursenkoina* sp.). These very small species usually live in low-oxygenated sediments, while *Ammonia* tolerate low-salinity conditions and potentially occur in mangrove habitats and estuaries with variable salinity conditions. All other benthic foraminifers are comparatively shallow marine, subtidal taxa, usually occurring in nearshore shallow-water environments characterized by algae or seagrass vegetation. The area was not hosting a typical reef or lagoon environment (absence of large symbiont-bearing foraminifers) and the open ocean influence was low. All 12 foraminifer species occur at the top of the KOU-AR6-05 section. With 90 individuals (71 in KOU-AR6-03), *Eponides repandus* is the most dominant foraminifer species in all trenches, like in the foraminifer associations observed in a mangrove estuary from northern Brazil, with a substantial marine influence through tides (28).

Table S7. Composition of KOU-AR6 foraminifer assemblages and individual abundances, earliest Late Pleistocene, Kourou, French Guiana.

Sample Number	<i>Quinqueloculina</i>	<i>Quinqueloculina</i> sp. 1	<i>Quinqueloculina</i> sp. 2	<i>Ammonia veneta</i>	<i>Ammonia tepida</i>	<i>Ammonia parkinsoniana</i>	<i>Elphidium magellanicum</i>	<i>Nonion subburgidum</i>	<i>Eponides repandus</i>	<i>Fursenkoina</i> sp.	<i>Cerebrina claricerviculata</i>	<i>Globigerina bulloides</i>
KOU-AR6-01 (Base)									3			
KOU-AR6-03 (Base)	2	1		14	11	1			71			
KOU-AR6-05 (Top)	5	3	2	3	1	1	2	5	8	1	1	1
KOU-AR6-06 (Base)								1	8			
Total number	7	4	2	17	12	2	2	6	90	1	1	1

3.3.2. Metazoans

Cnidarians

Cnidarians are documented by an octocorallian gorgonian (one specimen of *Pacifigorgia*, at KOU-AR6-06; Fig. 2G) and >1700 specimens of a single scleractinian species, *Astrangia rathbuni*, either growing as solitary corallites or small colonies (Fig. 2F). *Astrangia rathbuni* was recognized in all sampled marine levels, with a much higher density at KOU-AR6-06 than in other trenches. Solitary corallites dominate over colonies at KOU-AR6-06 and -05 Top, notably with respect to -03 (Base and Top) (*SI Appendix*, Table S8).

Table S8. Composition of KOU-AR6 *Astrangia rathbuni* assemblages, earliest Late Pleistocene, Kourou, French Guiana.

Locality	Layer	Sampled sediment (W) [kg]	Solitary	Colonial	Total (N)	Density (N/W)	Ratio (Solitary/total)
KOU-AR6-01	basal	>100	90	93	183	<1.83	0.49
KOU-AR6-03	basal	320	113	182	295	0.92	0.38
KOU-AR6-03	top	30	12	19	31	1.03	0.39
KOU-AR6-05	top	150	43	21	64	0.43	0.67
KOU-AR6-06	basal	255	804	353	1157	4.53	0.69
Total		>855	1062	668	1730	<2.02	0.61

Bryozoans

The trenches KOU-AR6-01, -03 and -05 yielded an unexpected taxonomic diversity of **bryozoans** mostly typical of tropical shallow waters, with 379 specimens assigned to 19 species, 12 genera and 11 families. Four species (*Biflustra arborescens*, *B. cf. savartii*, *Conopeum* sp. and *Steginoporella magnilabris*; Fig. 2H–J) occur in all sampled levels. More generally, bryozoans are much more abundant and diverse in the basal oyster-rich grey clays than in the khaki conglomerates (*SI Appendix*, Table S9). Most of these taxa also occur in the present-day coastal waters of Brazil [e.g., (29, 30)]. Warm-water genera (*Biflustra*, *Steginoporella*, *Antropora* and *Nellia*) are well represented in both recent and fossil Kourou records. The predominance of encrusting ‘anascans’ suggests a shallow depositional environment affected by freshwater influxes associated with increased turbidity, as in mangrove and oyster-rich settings (31). Among lophotrochozoans, around 200 calcareous tubes of unidentified polychaete worms are documented in the marine sequence of all trenches (half of the specimens do originate from (KOU-AR6-01).

Table S9. Composition of KOU-AR6 bryozoan assemblages, earliest Late Pleistocene, Kourou, French Guiana.

KOU-AR6-01 (basal oyster-rich grey clays)	KOU-AR6-03 (basal oyster-rich grey clays)	KOU-AR6-03 (kaki conglomerate)	KOU-AR6-05 (kaki conglomerate)	KOU-AR6-06 (basal oyster-rich kaki clays)	
<i>Antropora</i> sp.	1			<i>Anasca</i> indet. (small fragments)	3
<i>Biflustra arborescens</i>	119	63	22	<i>Biflustra arborescens</i>	8
<i>Biflustra</i> cf. <i>grandicella</i>	1				
		<i>Biflustra irregularata</i>	1		
<i>Biflustra marcusii</i>	1				
<i>Biflustra</i> cf. <i>savartii</i>	3	16	4	<i>Biflustra</i> cf. <i>savartii</i>	3
<i>Biflustra tenuis</i>	3				
				<i>Conopeum loki</i>	1
<i>Conopeum</i> sp.	20	12	2	<i>Conopeum</i> sp.	1
	<i>Conopeum</i> sp.				
	<i>Crisia</i> sp.	33			
<i>Ellisina</i> sp.	3				
<i>Membranipora</i> sp.	3		1		
	<i>Nellia tenella</i>	17			
				<i>Parasmittina</i> sp.	1
	<i>Quadracellaria</i> sp.	1			
	<i>Savignyella lafontii</i>	3			
	<i>Smittoidea</i> , fam. gen. et sp.	1			
<i>Steginoporella magnilabris</i>	14	10	2	<i>Steginoporella magnilabris</i>	3
	<i>Steginoporella magnilabris</i>	3			
	<i>Watersipora</i> sp.				
10 species	168	159	32	6 species	17
					1 species

specimens
379

Mollusks

Mollusks vastly dominate other phyla in both taxonomic diversity and specimen numbers (Fig. 2L–Y). They include two species of scaphopods (*Antalis antillarum* and *Dentalis laqueatum*; only a few shells), 35 species of bivalves and 50 species of gastropods. Bivalves and snails are recorded by thousands of individuals in all marine levels that were sampled, with shallow water *Costoanachis avara* (Fig. 2S), *Sheldonella bisulcata* (Fig. 2N), and *Chione cancellata* (Fig. 2W) most abundant. In terms of richness and evenness, KOU-AR6-03 is most diverse with 59 species (for 685 specimens), whereas KOU-AR6-06 yields only 30 species (for 1666 specimens; *SI Appendix*, Table S10). The state of preservation is exquisite for several specimens which retain colored patterns visible to the naked eye [e.g., *Vitta* (Fig. 2Q), *Pilsbryspira*] or revealed under UV light [e.g., *Crassinella*, *Olivella*; Fig. 2Y]. Most molluscan taxa have affinities to intertidal and shallow subtidal sands, muds, or rocks and several species are characteristic of mangrove habitats (e.g., *Vitta virginea*, *Isognomon radiatus*).

Table S10. Composition and abundance of KOU-AR6 molluscan assemblages, earliest Late Pleistocene, Kourou, French Guiana.

Class	Family	Species	KOU-AR6-01	KOU-AR6-03	KOU-AR6-05	KOU-AR6-06
Gastropoda	Amathinidae	<i>Iselica globosa</i>		1	15	110
Gastropoda	Ampullariidae	<i>Asolene</i> sp.	1			
Gastropoda	Ampullariidae	<i>Pomacea</i> sp.	1			
Gastropoda	Architectonicidae	<i>Heliacus bisulcatus</i>	40	5	28	68
Gastropoda	Buccinidae	<i>Engina turbinella</i>		X		
Gastropoda	Caecidae	<i>Caecum rhyssotitum</i>			5	
Gastropoda	Cerithiidae	<i>Bittium varium</i>				50
Gastropoda	Cerithiopsidae	<i>Cerithiopsis gemmulosum</i>		1	1	
Gastropoda	Cerithiopsidae	<i>Cerithiopsis</i> sp.		2		
Gastropoda	Cerithiopsidae	<i>Seila adamsii</i>			3	10
Gastropoda	Columbellidae	<i>Astyris lunata</i>		5	16	10
Gastropoda	Columbellidae	<i>Cosmioconcha</i> sp.	1			
Gastropoda	Columbellidae	<i>Costoanachis avara</i>	1	20	1	
Gastropoda	Columbellidae	<i>Parvanachis obesa</i>	1	120	108	200
Gastropoda	Cylichnidae	<i>Cylichna discus</i>		X		
Gastropoda	Epitoniidae	<i>Depressicala nitidella</i>	5	1		10
Gastropoda	Epitoniidae	<i>Gyroscala lamellosa</i>	80	4		150
Gastropoda	Eratoidae	<i>Archierato maugeriae</i>	1		1	
Gastropoda	Eulimidae	<i>Eulima bifasciata</i>	6	4	1	
Gastropoda	Fissurellidae	<i>Diodora cayenensis</i>	18	22		50
Gastropoda	Fissurellidae	<i>Lucapina sowerbii</i>	4			5
Gastropoda	Haminoeidae	<i>Cylichnella bidentata</i>		5	26	150
Gastropoda	Melongenidae	<i>Melongena melongena</i>		1		
Gastropoda	Muricidae	<i>Stramonita haemastoma</i>	1	4	6	8
Gastropoda	Nassariidae	<i>Phrontis vibex</i>		1		
Gastropoda	Naticidae	<i>Naticarius marochiensis</i>			1	X
Gastropoda	Naticidae	<i>Naticarius canrena</i>				X

Gastropoda	Naticidae	<i>Stigmaulax cayennensis</i>		6	1	X
Gastropoda	Naticidae	<i>Naticidae indet.</i>				14
Gastropoda	Neritidae	<i>Vitta virginea</i>	6	7	3	
Gastropoda	Olivellidae	<i>Olivella lactea</i>		25		
Gastropoda	Olivellidae	<i>Olivella minuta</i>	100	20		
Gastropoda	Olivellidae	<i>Olivella myrmecoon</i>		2		
Gastropoda	Ovulidae	<i>Pseudocyphoma intermedium</i>		2		
Gastropoda	Ovulidae	<i>Simnialena uniplicata</i>		2		
Gastropoda	Pyramidellidae	<i>Bonnea jadis</i>				50
Gastropoda	Pyramidellidae	<i>Chrysallida gemmulosa</i>		X		
Gastropoda	Pyramidellidae	<i>Pyrgolampros sp.</i>		1		100
Gastropoda	Pyramidellidae	<i>Turbonilla pusilla</i>			1	
Gastropoda	Pyramidellidae	<i>Turbonilla sp.</i>				60
Gastropoda	Pyramidellidae	<i>Turbonilla rixtae</i>		2		
Gastropoda	Pseudomelatomidae	<i>Pilsbryspira leucocyma</i>		3		
Gastropoda	Terebridae	<i>Impages cinerea</i>		1		7
Gastropoda	Terebridae	<i>Neoterebra dislocata</i>			8	
Gastropoda	Tornidae	<i>Cyclostremiscus sp.</i>			1	
Gastropoda	Triphoridae	<i>Monophorus olivaceus</i>			10	
Gastropoda	Triphoridae	<i>Triphora intermedia</i>		2		22
Gastropoda	Mangeliidae	<i>Kurtziella serga</i>		2		29
Gastropoda	Turridae	Turridae indet.				15
Gastropoda	Vermetidae	<i>Petalococonchus mcgintyi</i>			1	
Bivalvia	Anomiidae	<i>Pododesmus rudis</i>		1		
Bivalvia	Arcidae	<i>Acar domingensis</i>	2	8		3
Bivalvia	Arcidae	<i>Arca imbricata</i>	1			
Bivalvia	Arcidae	<i>Anadara chemnitzii</i>	1	1		
Bivalvia	Arcidae	<i>Cucullaearca candida</i>	1	1		2
Bivalvia	Arcidae	<i>Lunarca ovalis</i>	9	19	1	
Bivalvia	Cardiidae	<i>Dallocardia muricatum</i>	1	1		
Bivalvia	Chamidae	<i>Chama radians</i>	2	2		
Bivalvia	Corbulidae	<i>Caryocorbula contracta</i>	40	103	6	45
Bivalvia	Corbulidae	<i>Hexacorbula dietzana</i>		4		5
Bivalvia	Crassatellidae	<i>Crassinella lunulata</i>	33	2	1	75
Bivalvia	Dimyidae	<i>Dimya acuminata</i>		X		
Bivalvia	Isognomonidae	<i>Isognomon radiatus</i>		X		
Bivalvia	Leptonidae	<i>Lepton lepidum</i>		X		
Bivalvia	Mactridae	<i>Mulinia cleryana</i>	60	51	7	
Bivalvia	Mytilidae	<i>Gregariella chenui</i>		2		
Bivalvia	Mytilidae	<i>Brachidontes domingensis</i>		1		
Bivalvia	Noetiidae	<i>Arcopsis adamsi</i>		3	4	
Bivalvia	Noetiidae	<i>Sheldonella bisculcata</i>	23	83	10	120
Bivalvia	Nuculanidae	<i>Nuculana concentrica</i>	1	4		
Bivalvia	Nuculidae	<i>Ennucula puelcha</i>		1		
Bivalvia	Ostreidae	<i>Crassostrea rhizophorae</i>		10		3
Bivalvia	Pectinidae	<i>Argopecten gibbus</i>			1	
Bivalvia	Pectinidae	<i>Leptopecten bavayi</i>	56	23	4	95
Bivalvia	Plicatulidae	<i>Plicatula gibbosa</i>	2	46	1	50
Bivalvia	Pteriidae	<i>Pteria colymbus</i>		1		
Bivalvia	Semelidae	<i>Cumingia lamellosa</i>		1		
Bivalvia	Telinidae	<i>Angulus diantha</i>		2		
Bivalvia	Telinidae	<i>Eurytellina sp.</i>		1		
Bivalvia	Telinidae	<i>Strigilla sp.</i>		1		
Bivalvia	Telinidae	<i>Tampaella mera</i>		1		
Bivalvia	Thraciidae	<i>Asthenothaeus sp.</i>		1		
Bivalvia	Ungulinidae	<i>Diplodonta soror</i>		1		
Bivalvia	Veneridae	<i>Chione cancellata</i>	122	37	13	150
Bivalvia	Yoldiidae	<i>Orthoyoldia crosbyana</i>	1			
Scaphopoda	Dentaliidae	<i>Antalis antillarum</i>		1		
Scaphopoda	Dentaliidae	<i>Dentalium laqueatum</i>		1		

Arthropods

The crustacean arthropods are particularly dominant at Kourou, with thousands of specimens retrieved from the sediments, all belonging to either barnacles (balanomorph cirripeds), crabs or shrimps (decapods). The barnacles are represented by *Amphibalanus* sp. and an unidentified small balanid, with a large amount of disconnected wall plates found in all sampled localities, and a single complete

specimen (at KOU-AR6-01; Fig. 2Z). The decapods are represented mostly by hundreds of isolated claw remains, mainly of mobile and fixed fingers, with only a few other claw and carapace remains recovered. Decapod remains are much less abundant and poorly preserved in KOU-AR6-06 with respect to other trenches (*SI Appendix*, Table S11). The decapods comprise eight morphotypes, including two species of mud shrimps, three species of hermit crabs, and three species belonging to the true crabs. The mud shrimps, include ghost shrimps (*Neocallichirus* sp. (Fig. 2A'–B')) and Callichiridae indet. (Fig. 2C'–D'). Hermit crabs include porcelain crabs such as *Pachycheles* sp. (Fig. 2E') and *Petrolisthes* sp. (Fig. 2F'), which are filter feeders found in reefs, under rocks, shell beds, or mangroves. Small claw fragments further document a possible paguroid. The true crabs are represented by stone crabs (*Eriphia/Menippe*; Fig. 2G'–H'), crabs feeding on hard-shelled mollusks, including oysters. In addition, remains of the purse crab (?*Persephona* sp. (Fig. 2I')), and a swimming crab (Portunidae indet., Fig 2J') were found, but also small claw fragments of a spider crab (?*Majoidea* indet.) and a box crab (?*Hepatus* sp.). The overall decapod association indicates proximity to mangroves, with soft sediments hosting *Neocallichirus* mud shrimps (feeding on seagrass and algae) and purse crabs *Persephona*. This association points to intertidal–subtidal tropical to temperate waters (0–50 m), with Western Atlantic, Caribbean, and tropical Eastern Pacific affinities (*Persephona*).

Table S11. Composition of KOU-AR6 decapod crustacean assemblages, earliest Late Pleistocene, Kourou, French Guiana.

Clade/Superfamily/Family	Taxon	KOU-AR6	KOU-AR6-01	KOU-AR6-03	KOU-AR6-05	KOU-AR6-06	Total	Approx. ranges
Axiidea: Callichiridae	<i>Neocallichirus</i> sp.	125	637	700	8	18	1488	>1000
Axiidea: Callichiridae	Callichiridae indet.	28	23	10			61	10–100
Anomura: Galattheoidea: Porcellanidae	<i>Pachycheles</i> sp.		5	1			6	1–10
Anomura: Galattheoidea: Porcellanidae	<i>Petrolisthes</i> sp.		77				77	10–100
Anomura: Galattheoidea: Porcellanidae	Porcellanidae indet.	66	75	16			157	100–200
Anomura: Paguroidea	?Paguroidea indet.			1			1	1
Brachyura: Majoidea	? Majoidea indet.			1			1	1
Brachyura: Leucosioidea: Leucosiidae	? <i>Persephona</i> sp.		1	1			2	1–5
Brachyura: Aethroidea: Aethridae	? <i>Hepatus</i> sp.		1				1	1
Brachyura: Portunoidea: Portunidae	Portunidae indet.	8	23	16		5	52	10–100
Brachyura: Eriphioidea	<i>Eriphia/Menippe</i>	60	35	64	11	73	243	100–500

Echinoderms

Echinoderms were retrieved in high numbers in all marine samples, nevertheless pointing to a low taxonomic diversity (three species). The echinoderm community is overdominated by the Atlantic purple sea urchin (*Arbacia punctulata*; Fig. 2K), easily recognizable through 1985 spines, but also by 138 jaw and test fragments from all sampled levels and trenches (*SI Appendix*, Table S12). In stark contrast, other echinoderm specimens include only a few dozens of test fragments of two unidentified heart urchins (one and 67 specimens) and two plates of an astropectinid sea star, sampled in the basal grey level at KOU-AR6-01 and in the khaki conglomerate at KOU-AR6-03 (Top).

Table S12. Composition of KOU-AR6 echinoderm assemblages, earliest Late Pleistocene, Kourou, French Guiana.

<i>Taxon</i>	<i>comments</i>	KOU-AR6-01 grey clays	KOU-AR6-03 grey oyster-rich clays	KOU-AR6-03 kaki conglomerate	KOU-AR6-05 kaki conglomerate (top)	KOU-AR6-06 basal clays	Total specimens per taxon
<i>Arbacia punctulata</i>	Fragments of sea urchin jaw (hemipyramid)		12	13		1	2123
	Fragments of sea urchin jaw (rotula)			3			
	Fragments of sea urchin jaw (epiphysis)			1		1	
	Complete primary spines	76	251	325	49	225	
	Fragments of primary spines	256	20	82	41	660	
	Test fragments (Ambulacral and interambulacral plates)	34		54	2	17	
Spatangoida indet. 1	Test fragments (Ambulacral and interambulacral plates)			1			1
Spatangoida indet. 2	Test fragments (Ambulacral and interambulacral plates)	52		15			67
Astropectinidae indet.	Inferomarginal plate	1		1			2
Total specimens per sampling locality		419	283	495	92	904	2193

Elasmobranchs

Sharks, rays and saw fish (elasmobranchs) and bony fish were found and identified (i.e., no marine mammals or seabirds). All trenches have yielded a total of 110 isolated teeth of elasmobranchs (Fig. 2L'–O'), with four genera and families of rays (*Hypanus whipray*, *Aetobatus* eagle ray, *Pristis* saw fish, and *Rhinoptera* cownose ray) and seven species of sharks, among which five requiem sharks (*Carcharhinus* sp. and smalltail shark, *Carcharhinus porosus*; daggernose shark, *Isogomphodon oxyrhynchus*; sharpnose shark, *Rhizoprionodon* sp.; lemon shark, *Negaprion brevirostris*), a small hammer shark (scoophead, *Sphyrna media*) and a nurse shark (*Ginglymostoma cirratum*). Daggernose sharks and whiprays dominate the elasmobranch fauna in terms of specimens and occurrences (present in all sampling levels for the former [24%], in all but the trench KOU-AR6-01 for the latter [32%]; *SI Appendix*, Table S13).

Table S13. Composition of KOU-AR6 elasmobranch assemblages, earliest Late Pleistocene, Kourou, French Guiana.

	KOU-AR6-01 Grey conгло (base)	KOU-AR6-02 Grey conгло (base)	KOU-AR6-03 Grey clay (base)	KOU-AR6-03 Kaki conгло (top)	KOU-AR6-05 Kaki conгло (top)	KOU-AR6-06 Grey clays (base) >2mm	KOU-AR6-06 Grey clays (base) <2 mm	KOU-AR6-06 Kaki clays (top)	Total number per taxon	Order	Family	Common name	IUCN status
<i>Hypanus</i> sp.		3	8	5	2	4	12	1	35	Myliobatiformes	Dasyatidae	whipray	least concern-near threatened
<i>Aetobatus</i> sp.	1		1			2	2		6	Myliobatiformes	Myliobatidae	eagle rays	endangered (<i>A. narinari</i>)
<i>Rhinoptera</i> sp.				1			1		2	Myliobatiformes	Rhinopteridae	cownose rays	vulnerable
<i>Pristis</i> sp.		1							1	Rhinopristiformes	Pristidae	sawfish	critically endangered-endangered
<i>Carcharhinus porosus</i>	2					1	5		8	Carcharhiniformes	Carcharhinidae	smalltail shark	critically endangered
<i>Carcharhinus</i> sp.						1			1	Carcharhiniformes	Carcharhinidae	-	least concern-critically endangered
<i>Isogomphodon oxyrhynchus</i>	1	1	10	1	2	5	5	1	26	Carcharhiniformes	Carcharhinidae	daggernose shark	critically endangered
<i>Rhizoprionodon</i> sp.		?	2		1	2	2	1	6	Carcharhiniformes	Carcharhinidae	sharpnose sharks	vulnerable-near threatened
<i>Negaprion brevirostris</i>			2			2			4	Carcharhiniformes	Carcharhinidae	lemon shark	vulnerable
<i>Sphyrna media</i>	1		1			9	5		16	Carcharhiniformes	Sphyrnidae	scoophead	critically endangered
<i>Ginglymostoma cirratum</i>			1		1	2	1		5	Orectolobiformes	Ginglymostomatidae	nurse shark	vulnerable
Subsamples	5	5	25	7	6	26	33						
Number per locus	5	5	25	7	6	59	3		110				

Actinopterygians

Bony fish are mostly documented by otoliths (478 were identified; Fig. 2P'–T'), but also by bones and teeth (Fig. 2U'–W'), belonging to 35 species, 26 genera and 12 families (*SI Appendix*, Table S14). Sciaenid perciforms (16 species and 10 genera, with five species and 212 specimens of *Stellifer*) and ariid siluriforms (eight species, with *Cathorops spixii* [104 otoliths] and *Aspistor luniscutis* [44 otoliths]) widely outnumber other taxonomic groups in the sample. KOU-AR6-03 is by far the richest locality, with 425 specimens documenting 32 species, whereas taxonomic diversity is lower in KOU-AR6-01, -05 and -06, (7–10 species for only 10–38 specimens; *SI Appendix*, Table S14). The sciaenid *Macrodon ancylodon* occurs in all four localities, whereas 13 species are recognized in two or three localities, pointing to spatiotemporal homogeneity between the samples.

Table S14. Composition of KOU-AR6 bony fish assemblages, earliest Late Pleistocene, Kourou, French Guiana. Number of specimens per trench and sampled level. In red, bone and/or dental record. In black, otolith record. In bold, total number of specimens per taxon. Blue cells, marine taxa; yellow cells, freshwater taxa; green cells, marine, brackish, and freshwater taxa.

Order	Family	Species	AR6-01	AR6-03	AR6-05	AR6-06	Total	
Albuliformes	Albulidae	<i>Albula vulpes</i>				1	1	
Anguilliformes	Nettastomatidae	Gen. et. sp. indet.		1			1	
Batrachoidiformes	Batrachoididae	<i>Thalassophryne</i> sp.		2	2		4	
		Gen. et. sp. indet.			2		2	
Characiformes	Erythrinidae	cf. <i>Hoplias</i>		4		3	7	
Clupeiformes	Engraulidae	<i>Anchoa</i> sp.		6	3		9	
Perciformes	Centropomidae	cf. <i>Centropomus</i>		1			1	
	Carangidae	cf. <i>Selene</i>		1			1	
	Sciaenidae	<i>Cynoscion acoupa</i>			2			2
		<i>Isopisthus parvipinnis</i>			1			1
		<i>Larimus breviceps</i>			3			3
		<i>Lonchurus lanceolatus</i>			5			5
		<i>Macrodon ancylodon</i>		1	25	4	3	33
		<i>Macrodon atricauda</i>			1			1
		<i>Micropogonias furnieri</i>			1			1
		<i>Nebris microps</i>			6	1	1	8
		<i>Ophioscion punctatissimus</i>			1			1
		<i>Ophioscion</i> sp.			1			1
		<i>Paralonchurus brasiliensis</i>			1			1
		<i>Stellifer brasiliensis</i>			2		1	3
		<i>Stellifer menezzi</i>				4		4
<i>Stellifer gomezi</i>			1			1		
<i>Stellifer rastrifer</i>			143	5	5	153		
<i>Stellifer</i> sp.			2			2		
<i>Stellifer</i> (lapilli)			1	44		4	49	
Scorpaeniformes	Scorpaenidae	Gen. et. sp. Indet.		1			1	
Siluriformes	Ariidae	<i>Aspistor quadriscutis</i>	3	2	6		11	
		<i>Aspistor luniscutis</i>		40	3	1	44	
		<i>Bagre bagre</i>		17			17	
		<i>Bagre marinus</i>		1			1	
		<i>Cathorops higuchii</i>	1		8		9	
		<i>Cathorops spixii</i>	1	101		2	104	
		<i>Notarius grandicassis</i>	1	2			3	
		Gen. et. sp. indet.	2	5		2	2/7	
	Non-Ariidae	Gen. et. sp. indet.		1			1	
Synbranchiformes	Synbranchidae	<i>Synbranchus</i> sp.		1			1	
		N specimens	10	425	38	23	496	
otoliths	bones	N taxa	7	32	10	10	35	
marine	freshwater	marine/freshwater						

3.3.3. Plantae

Charcoal

Unit A: From the bottom of the marine sequence (basal oyster-rich grey clays), 99 charcoals were hand-picked. Vitrification and/or poor preservation hampered taxonomic assignment of all charcoals from KOU-AR6-05 (khaki clays) and -06 trenches (Base, Top). Yet, cf. *Rhizophora* sp. (red mangrove, Rhizophoridae), cf. *Symphonia globulifera* (boarwood, Clusiaceae) and two representatives of Chrysobalanaceae and Myrtaceae were recognized at KOU-AR6-01, as well as branch and twig fragments of cf. *Rhizophora* sp. at KOU-AR6-03 (*SI Appendix*, Table S15).

Unit B: Tree charcoals were identified at KOU-AR6-04 Base (Fig. 3Y; *SI Appendix*, Table S15). The assemblage comprises notably *Hadroanthus* cf. *serratifolius* (ipê) and a close relative, cf. *Drypetes* sp., *Pterocarpus*-like Leguminosae, red mangrove, as well as unidentified Melastomataceae, Myrtaceae-like dicots. Today, these taxa represent trees and shrubs from the primary, riverine or dry forest, savanna or mangrove and suggest distinct vegetation succession stages at ca. 47 ka cal BP.

Unit C: Macroscopic charcoals were hand-picked at KOU-AR6-04, in several levels from Unit C, spanning the 47–1 ka time interval (MIS 3c–1). More than 60 fragments, some of them from tree stumps, were retrieved in a brown conglomerate ("Mid"), ¹⁴C-dated at 47053±572 cal BP. They attest to the most speciose tree community uncovered here through charcoal, with at least 15 distinct tree taxa (*SI Appendix*, Table S15). *Mouriri* sp. (Melastomataceae) is the most abundant, followed by *Chaunochiton kappleri* and a close relative (Olacaceae), two close allies of *Stryphnodendron* (Leguminosae), two unidentified Chrysobalanaceae, Lecythidaceae, cf. Anacardiaceae/Burseraceae and *Hadroanthus capitatus/serratifolius* (ipê). Just above, floodplain deposits and a silty litter dated at 43091±284 cal BP yielded charcoals of unidentified affinities and *Eperua* cf. *falcata* (bootlace tree, Leguminosae), respectively. The top levels, dated from the last millennia (¹⁴C ages of 1938±120 and 804±55 cal BP), yield charcoals of unidentified Anacardiaceae/Burseraceae, hog plum (cf. *Spondias mombin*), cf. Chrysobalanaceae, *Mabea* sp. (Euphorbiaceae) in the older layer and *Eperua* cf. *falcata* (27 chunks), Rubiaceae anatomically close to *Capirona decorticans* (Batahua, 13 chunks), as well as unidentified Chrysobalanaceae and Leguminosae in the younger one.

Table S15. Composition of KOU-AR6 macrocharcoal assemblages, earliest Late Pleistocene, Kourou, French Guiana.

Taxon	Unit A					Unit B	Unit C				
	KOU-AR6-01 (10/2018, 02/2019, 04/2019)	KOU-AR6-03 (04/2019)	KOU-AR6-05, Kaki clays (04/2019)	KOU-AR6-06, Base (10/2021)	KOU-AR6-06, Top (10/2021)	KOU-AR6-04, Base	KOU-AR6-04, Mid	KOU-AR6-04, Silt litter	KOU-AR6-04, C14-1	KOU-AR6-04, Top	KOU-AR6-04, C14-2
Anacardiaceae/Burseraceae										1	
cf. Anacardiaceae/Burseraceae							1				
<i>Chaunochiton kappleri</i>							4				
cf. <i>Chaunochiton kappleri</i>							3				
Chrysobalanaceae	2						2			6	
cf. Chrysobalanaceae	2						4		2		
cf. <i>Drypetes</i> sp.						1					
<i>Eperua</i> cf. <i>falcata</i>								3		27	
<i>Handroanthus capitatus/serratifolius</i>							1				
<i>Handroanthus</i> cf. <i>serratifolius</i>						1					
Type <i>Handroanthus</i>						4					
type Lecythidaceae							2				
Leguminosae type 1										1	
Leguminosae type 2							1				
<i>Mabea</i> sp.									1		
Melastomataceae						1					
<i>Mouriri</i> sp.							10				
cf. Myrtaceae	1					1					
Type <i>Pterocarpus</i>						1					
<i>Rhizophora</i> sp.						3					
cf. <i>Rhizophora</i> sp.	1	4									
cf. Rubiaceae (<i>Capirona decorticans</i>)											13
cf. <i>Spondias mombin</i>									2		
Leguminosae, type <i>Stryphnodendron</i>							1				
cf. <i>Symphonia globulifera</i>	2										
Unidentified 1	1										
Unidentified 2	1										
Unidentified 3	1										
Unidentified 4		1									
Unidentified 5										11	
Unidentified 6										2	
Unidentified 7										1	
Unidentified 8							1				
Unidentified 9							1				
Unidentified 10							1				
Unidentified 11							1				
Unidentified 12						1					
Unidentified 13						1					
Unidentifiable	27	17	4	24	11	34	29	4		42	

Total number of specimens	38	22	4	24	11	48	62	4	3	62	47	325
Minimum number of species/level	9	3	1	1	1	10	15	1	1	8	5	39
Minimum number of species/sequence	10					10	24					

Phytoliths

Unit A: At KOU-AR6-06, the base of the Unit A yielded phytoliths referable to unidentified woody eudicot and Asteraceae (in PN9A and PN9C pollen samples, respectively). The corresponding palynological assemblage (Fig. 3A–I), with a low pollen concentration (around 700 grains.cm⁻³), is dominated by *Rhizophora* pollen (80 %), followed by spores of the mangrove fern *Acrostichum* (3.5 %). No *Avicennia* pollen were found. Pollen of tree species account for 9 % of the pollen sum, and reflect the influx of hinterland (Podocarpaceae, *Alnus*) and lowland (swamp) forest trees [e.g., *Iriartea*, *Catostemma* and *Symphonia* (32)]. Herb and vine pollen is relatively rare (5 %) and dominated by Poaceae and Asteraceae. Asteraceae pollen grains were only found in the PN9C sample, also containing one Asteraceae phytolith. The top of this unit has been comprehensively sampled at KOU-AR6-06 for palynomorphs and phytoliths (samples PN10–14; *SI Appendix*, Table S16). PN10–13 only provided a few phytoliths and PN10–14 was also devoid of palynological content. Grass phytoliths first occur at PN12 (dated at 104.6±17.9 ka, OSL-2), with a panicoid cross and a bilobate [C3 and C4 grasses (33, 34)], plus a fused and two rugose spheroids (woody eudicots). PN14 yielded phytolith assemblages dominated by grass phytoliths (70%), as in PN15A-B (base of Unit B, see below). PN14 had a lower concentration (<50 phytoliths) than the latter sample.

Unit B: The phytolith assemblages counted in the basal dark peat at KOU-AR6-06 (Fig. 3R –X) are dominated by grasses (65%) in both PN15A and PN15B with 65% grass, 31 and 17% woody eudicots, respectively, and almost no palm phytoliths (<1%). Most grass phytoliths encountered are from Panicoideae and Bambusoideae (*SI Appendix*, Table S16; Fig. S12). Bilobates and rondels are also common, produced by a wide array of monocot grasses (33, 34). Phytoliths from Pooideae (wavy trapezoids) and Chloridoideae (squat saddles) are rare (<1%). Strikingly, a high percentage of phytoliths were burnt (28%), especially specimens of Cyperaceae, *Heliconia* and Zingiberales. This assemblage suggests that a savanna vegetation had started growing locally way before 50 ka and spread around and settled sustainably. Previous phytolith studies showed that the natural vegetation of seasonally-flooded/coastal Holocene savannas in French Guiana consisted of Cyperaceae, Marantaceae and *Heliconia* herbs and panicoid and oryzoid grasses, with an overall high abundance of grass phytoliths (35).

Unit C: The absence of phytolith and pollen record in Unit C impedes characterizing further the last pre-Columbian seasonally-flooded local savannas (36).

Table S16. Phytolith recovery from PN9–15 samples (latest Middle and Late Pleistocene), KOU-AR6-06, near the ELA4 Ariane 6 launcher pad, Kourou, French Guiana.

Site_name	Burned_phytoliths	Heliconia	Pooideae	Pharoidae	Other_palms	Conical	Spheroid	Rugose	Nodular	Ornate	Psilate	Other_Arboreal	Woody_dicots (=sum(rugose, ornate, other_arboreal))	Cyperaceae	Zingiberales (druses)	Panicoideae	Bambusoideae	Chloridoideae	Rondels	Other_grasses	Bilobates	Cross	Oryzoideae
KOU-ARG-06-PN15B	32,08	2,73	-	-	-	0,21	-	14,05	-	0,63	2,10	0,21	14,88	1,89	0,21	26,42	19,71	-	9,43	2,73	16,35	1,89	-
KOU-ARG-06-PN15A	24,45	2,44	0,24	-	-	-	-	20,54	-	2,20	6,60	1,47	24,21	1,47	0,24	14,18	8,56	0,24	7,82	3,91	28,61	0,49	-
PN15AB average	28,26	2,59	0,12	-	-	0,10	-	17,29	-	1,41	4,35	0,84	19,55	1,68	0,23	20,30	14,13	0,12	8,63	3,32	22,48	1,19	-

Site Name	Countable?	Phytoliths?	Diatoms?
KOU-ARG-06 PN15B	yes	17% arboreal, 65% grasses. Burnt Cyperaceae and Heliconia present. Mostly Panicoideae, few Bambusoideae	yes
KOU-ARG-06 PN15A	yes	31% arboreal, 65% grasses. Burnt Cyperaceae and Heliconia present. Mostly Panicoideae, few Bambusoideae, Pooideae, Chloridoideae	yes
KOU-ARG-06 PN14	no, but up to ±50 phytoliths	Similar to PN15A-B	no
KOU-ARG-06 PN13	no	1 ornate spheroid and 1 rugose spheroid (woody dicots)	no
KOU-ARG-06 PN12	no	1 fused spheroid, 2 rugose spheroids (woody dicots), 1 bilobate and 1 Panicoid cross 2	no
KOU-ARG-06 PN11	no	1 rugose spheroid (woody dicot)	no
KOU-ARG-06 PN10	no	few non-diagnostic phytoliths only (tracheids/bulliforms)	no
KOU-ARG-06 PN9D	no	-	no
KOU-ARG-06 PN9C	no	Asteraceae	no
KOU-ARG-06 PN9B	no	-	no
KOU-ARG-06 PN9A	no	1 rugose spheroid (woody dicot)	no

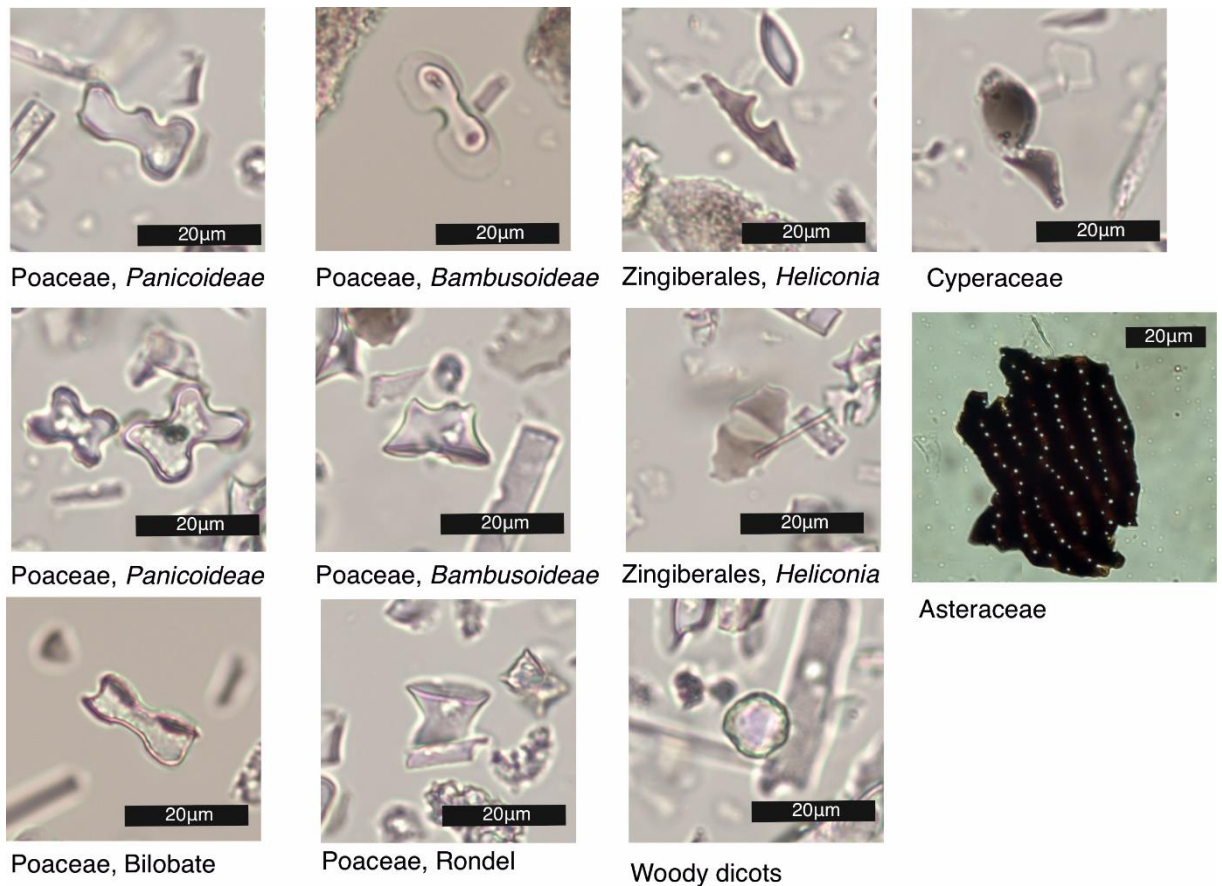


Fig. S12. Selected phytoliths from PN15 (Late Pleistocene), KOU-AR6-06, near the ELA4 Ariane 6 launcher pad, Kourou, French Guiana.

Pollen

Unit A: The sample PN6, located at 1.4 m ASL, yielded high amounts of *Rhizophora* mangrove pollen, including clumps, which suggest the proximity of a mangrove belt.

Unit B: The pollen concentration of the PN15 sample is much higher than in Unit A (around 20,600 grains.cm⁻³), with a high relative abundance of Poaceae (49 %) and Spermacoceae (36 %) pollen, indicators of open and disturbed vegetation (Fig. 3L–Q) prior to 45 ka *cal* BP in the ELA4 area (Fig. 4B). Many Poaceae pollen grains are relatively large (50–64 µm), furthering the presence of Panicoideae and Bambusoideae grass phytoliths. Mangrove (2.4 %) and tree (3.5 %) pollen are rare (*SI Appendix*, Table S17). Conversely, the large amount of charred plant fragments (“microcharcoals”) in the pollen slides is notable. The high number of macro-charcoals and high percentage of burned phytoliths indicate recurring fires at the site during the concerned time interval, i.e., prior to 47 ka *cal* BP (age of the base of the overlying Unit C; see below), and further consistent with a glacial stadial (MIS 4: 72–58 ka; Fig. 4).

Unit C: The absence of phytolith and pollen record in Unit C impedes characterizing further the last pre-Columbian seasonally-flooded local savannas (36).

Table S17. Composition of KOU-AR6-06 pollen assemblages, early Late Pleistocene, Kourou, French Guiana.

KOU-AR6				KOU-AR6-PN9 (%)		KOU-AR6-PN15 (%)	
		Lycopodium/cm3		18407		18407	
		Lycopodium		8650		334	
		pollen sum		323		374	
		pollen conc. (grains/cm3)		687		20611	
group							
1	Acanthaceae	<i>Avicennia</i>	mangrove, tree	0	0,0	0	0,0
1	Pteridaceae	<i>Acrostichum</i>	mangrove, fern	11	3,4	0	0,0
1	Rhizophoraceae	<i>Rhizophora</i>	mangrove, tree	257	79,6	9	2,4
2	Areaceae	<i>Attalea</i> type	palm tree	3	0,9	1	0,3
2	Areaceae	<i>Iriatea</i>	palm tree	1	0,3	0	0,0
2	Areaceae	<i>Prestoea</i> type	palm tree	1	0,3	0	0,0
3	Anacardiaceae	undiff.	tree	1	0,3	0	0,0
3	Aquifoliaceae	<i>Ilex</i>	tree	1	0,3	0	0,0
3	Araliaceae	<i>Schefflera</i>	tree	1	0,3	1	0,3
3	Betulaceae	<i>Alnus</i>	tree	1	0,3	0	0,0
3	Burseraceae	<i>Protium</i>	tree	3	0,9	0	0,0
3	Chloranthaceae	<i>Hedyosmum</i>	tree	3	0,9	0	0,0
3	Clusiaceae	<i>Symphonia</i>	tree	1	0,3	0	0,0
3	Euphorbiaceae	<i>Mabea</i>	tree	0	0,0	1	0,3
3	cf. Malpighiaceae	<i>Byrsonima</i>	tree	0	0,0	7	1,9
3	Malvaceae	<i>Catostemma</i>	tree	1	0,3	0	0,0
3	Malvaceae	<i>Pachira</i>	tree	0	0,0	0	0,0
3	Melastomataceae	<i>Mouriri</i>	tree	1	0,3	0	0,0
3	cf. Meliaceae	<i>Trichilia</i>	tree	2	0,6	0	0,0
3	Myristicaceae	<i>Virola</i>	tree	0	0,0	0	0,0
3	Myrtaceae	undiff.	tree	6	1,9	1	0,3
3	Podocarpaceae	<i>Podocarpus</i>	tree	1	0,3	0	0,0
3	Polygonaceae	<i>Symmeria</i>	tree	0	0,0	0	0,0
3	Urticaceae	<i>Cecropia</i>	tree	0	0,0	0	0,0
3	Urticales	undiff.	tree	1	0,3	0	0,0
4	Asteraceae	undiff.	herb	4	1,2	29	7,8
4	Asteraceae	<i>Vernonia</i> type	herb	0	0,0	0	0,0
4	Convolvulaceae	<i>Ipomoea</i>	herb/vine	0	0,0	0	0,0
4	Euphorbiaceae	<i>Acalypha</i>	herb	1	0,3	0	0,0
4	Gentianaceae	<i>Schultesia</i>	herb	0	0,0	1	0,3
4	Malvaceae	<i>Peltaea</i>	herb/vine	3	0,9	0	0,0
4	Poaceae	undiff.	herb	6	1,9	186	49,7
4	Rubiaceae	Spermacoceae	herb	0	0,0	137	36,6
4	Verbenaceae	<i>Petrea</i>	herb/vine	1	0,3	0	0,0
5	Apiaceae	undiff.	undefined	1	0,3	1	0,3
5	Bignoniaceae	undiff.	undefined	1	0,3	0	0,0
5	Fabaceae (P)	undiff.	undefined	1	0,3	0	0,0
5	Malpighiaceae	undiff.	undefined	3	0,9	0	0,0
	Melastomataceae/						
5	Combretaceae	undiff.	undefined	1	0,3	0	0,0
5	Proteaceae	undiff.	undefined	0	0,0	0	0,0
5	cf. Rubiaceae	<i>Alseis</i>	undefined	2	0,6	0	0,0
5	Rutaceae	undiff.	undefined	1	0,3	0	0,0
5	Salicaceae	undiff.	undefined	2	0,6	0	0,0
		mangrove		█	83,0	█	2,4
		trees		█	8,7	█	2,9
		herbs/vines		█	4,6	█	94,4
		undefined		█	3,7	█	0,3
		total			100,0		100,0

4. Recent referential for marine taxonomic diversity of metazoans



Fig. S13. Map of the sampling survey for recent marine invertebrates and bony fish, performed in 1954–1957 on the Guianese continental plate. Four hundred samples were caught on a ca. 40,000-km² area and at a 0–105-m depth, among which 66 and 234 samples at 0–24 and 25–49-m depth ranges, respectively. Sampling areas coincide with those depicted by (37). Background from Google Earth®.

Table S18. Comparison of taxonomic diversity per metazoan group, between the 1954–1957 survey on recent organisms [(37); see **Fig S13** above] and the Kourou ELA4 sampling effort, in the early Late Pleistocene of Kourou, French Guiana (this work), detailing species/generic diversity depending on the depth range (between brackets) and type of substrate, when available. Mud: 0–30-m depth, 110 samples; muddy sands: 20–49-m depth, 272 samples; dead shells: 20–49-m depth, 272 samples; sands: 20–49-m depth, 272 samples; Last Interglacial (LIG) diversity is measured through five samples from a 0.5 km² area. White/yellow/green cells denote lower/similar/higher diversity between LIG and recent samples.

Taxonomic groups	Recent diversity (Guianese continental plate): species/genera				LIG diversity	
	mud (0-30 m)	muddy sands (20-49 m)	dead shells (20-49 m)	sands (20-49 m)	muddy sands (5-10 m)	
Corals	0/0	1/1		1/1		
Mollusks	Gastropods	13/11			50/44	
	Bivalves	20/16			35/35	
	Scaphopods	1/1			2/2	
Decapods	Brachyurans	10/7	-	5/5	8/8	5/5
Echinoderms	Sea stars	2/2	4/3	4/3	4/3	1/1
	Urchins	0/0	0/0	4/4	3/3	3/3
Bony fish	35/31	40/37	41/35	30/26	35/26	
Total	81/68	79/69	89/76	80/69	132/117	

5. PAUP Buffer

P A U P *

Version 4.0a (build 169) for 32-bit Microsoft Windows (built on Feb 10 2021 at 22:12:44)

Thu Dec 28 16:29:05 2023

-----NOTICE-----

This is a test version that is still changing rapidly.
Please report bugs to dave@phylosolutions.com

Running on Intel(R) Core(TM) i5-7200U CPU @ 2.50GHz

Current processor contains 2 CPU cores on 1 socket (hyperthreaded to 4 logical cores)

Executable built for IA-32 architecture (64-bit word length)

SSE vectorization enabled

SSSE3 instructions supported

Multithreading enabled using Pthreads

Processing of file "C:\Users\pierr\Documents\Publications\En cours\Kourou ELA4
assemblage\R2\Antoine-et-al_SI-Appendix4_R2.nex" begins...

Data matrix has 7 taxa, 74 characters

Valid character-state symbols: 01

Missing data identified by '?'

Gaps identified by '-'

*** Skipping "NOTES" block

Processing of input file "Antoine-et-al_SI-Appendix4_R2.nex" completed.

paup> set criterion=distance;

Optimality criterion set to distance.

paup> UPGMA;

UPGMA search settings:

Ties (if encountered) will be broken systematically

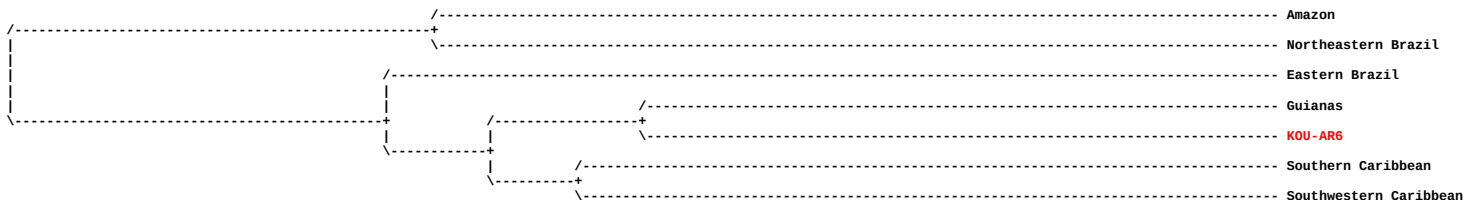
Distance measure = mean character difference

74 characters are included

All characters have equal weight

(Tree is rooted)

UPGMA tree:



Tree found by UPGMA method stored in tree buffer

Time used for tree calculation = 0.00 sec (CPU time = 0.00 sec)

paup> set criterion=parsimony;

Optimality criterion set to parsimony.

paup> set rootMethod=midpoint;

paup> allTrees;

Exhaustive search settings:

Optimality criterion = parsimony

Character-status summary:

Of 74 total characters:

All characters are of type 'unord'

All characters have equal weight

3 characters are constant (proportion = 0.0405405)

14 variable characters are parsimony-uninformative

Number of parsimony-informative characters = 57

Gaps are treated as "missing"

Initial 'Maxtrees' setting = 100

Branches collapsed (creating polytomies) if maximum branch length is zero

'MulTrees' option in effect

No topological constraints in effect

Trees are unrooted

Exhaustive search completed:

Number of trees evaluated = 945

Score of best tree found = 117

Score of worst tree found = 153

Number of trees retained = 1

Time used = 0.00 sec (CPU time = 0.00 sec)

paup> describeTrees;

Tree description:

Unrooted tree(s) rooted using midpoint method

Optimality criterion = parsimony

Character-status summary:

Of 74 total characters:

All characters are of type 'unord'

All characters have equal weight

3 characters are constant (proportion = 0.0405405)

14 variable characters are parsimony-uninformative

Number of parsimony-informative characters = 57

Gaps are treated as "missing"

Character-state optimization: Minimum F-value (MINF)

Tree 1 (rooted using midpoint method)

Tree length = 117

Consistency index (CI) = 0.6068

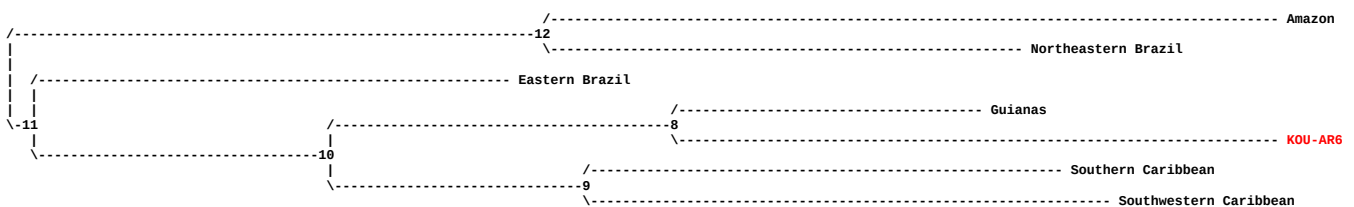
Homoplasy index (HI) = 0.3932

CI excluding uninformative characters = 0.5534

HI excluding uninformative characters = 0.4466

Retention index (RI) = 0.4713

Rescaled consistency index (RC) = 0.2860



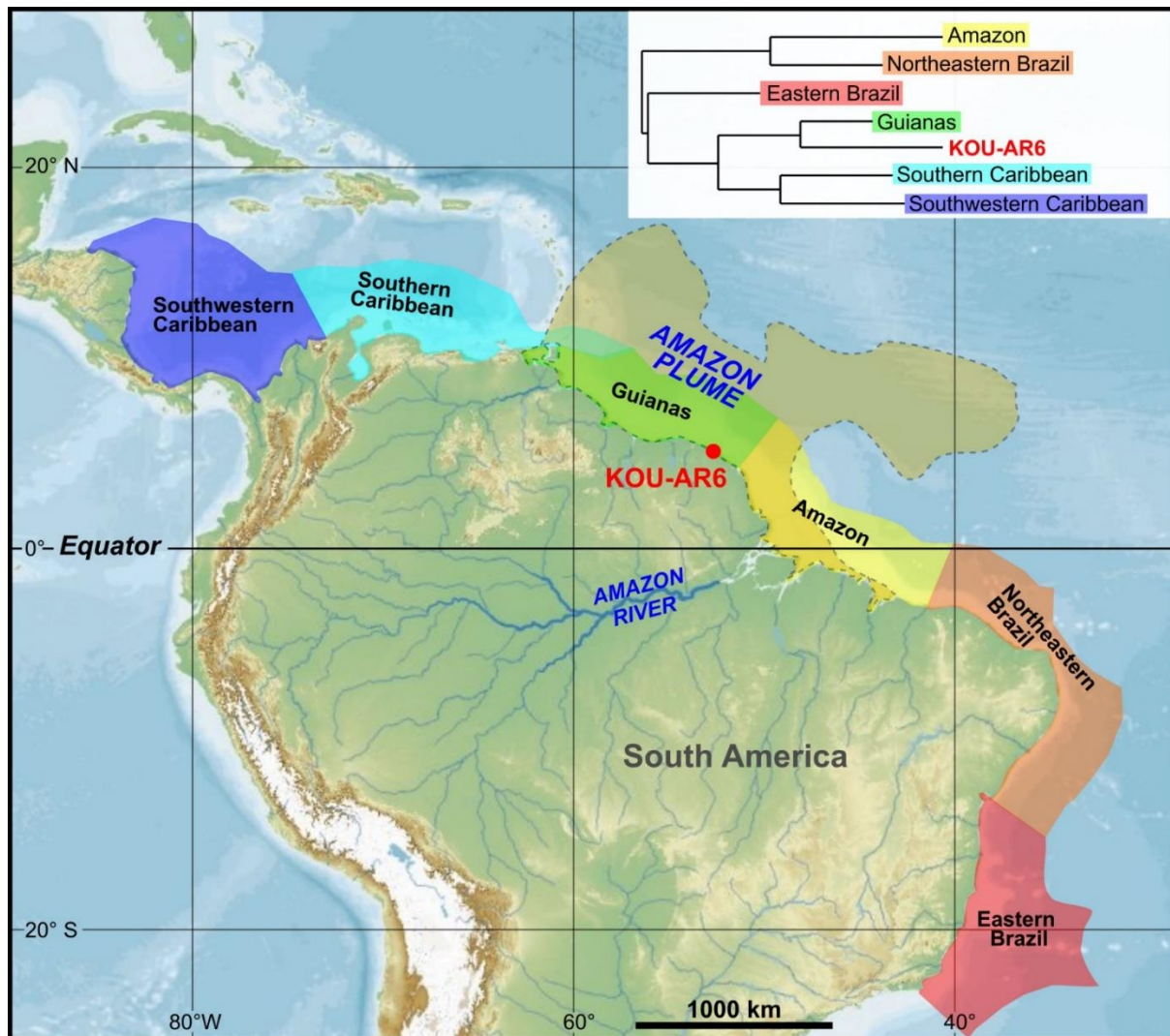


Fig. S14. Biogeographic map of the tropical Western Atlantic with coastal areas considered in Giachini Tosetto et al. (38) and taxon-related data extracted from both Ocean Biodiversity Information System repository (<https://mapper.obis.org>), the Malacolog Version 4.1.1 Database (<http://www.malacolog.org/wasp.php?mode=locality>) of Western Atlantic Marine Mollusca, and a monograph on French Guiana’s mollusks (39). Superimposed white box stands for cluster dendrogram analysis depicting the overall similarity between the Last Interglacial KOU-AR6 fossil mollusk assemblage and the recent mollusk communities from six contiguous coastal areas of the tropical Western Atlantic. The corresponding topology was obtained through distance analysis (UPGMA) and parsimony analysis (using mid-point rooting method). Ecological conditions were more similar between KOU-AR6 and the Guianas, and the Southern + Southwestern Caribbean, than with Eastern Brazil and, to a wider extent, with Northeastern Brazil and Amazon coastal waters today. This pattern suggests that the Amazon Plume was not acting as a strong ecological barrier in coastal areas of the Guianese continental shelf by Last Interglacial times, in stark contrast to today’s pattern.

SI References

1. R. Scheel-Ybert, Charcoal collections of the world. *IAWA Journal* **37**, 489–505 (2016).
2. InsideWood, Published on the Internet. (2004-onwards). [<http://insidewood.lib.ncsu.edu/search>; accessed in July 2020].
3. E. A. Wheeler, Inside Wood—A web resource for hardwood anatomy. *Iawa Journal* **32**, 199–211 (2011).
4. S. C. Bodin, et al., CharKey: An electronic identification key for wood charcoals of French Guiana. *IAWA Journal* **40**, 75–S20 (2019).
5. C. N. H. McMichael et al., 30,000 years of landscape and vegetation dynamics in a mid-elevation Andean valley. *Quatern. Sci. Rev.* **258**, 106866 (2021).

6. C. Crifò, C.A. Strömberg, Small-scale spatial resolution of the soil phytolith record in a rainforest and a dry forest in Costa Rica: applications to the deep-time fossil phytolith record. *Palaeogeogr., Palaeoclimatol., Palaeoecol.* **537**, 109107 (2020).
7. K. Neumann *et al.*, International Code for Phytolith Nomenclature (ICPN) 2.0. *Ann. Botany* **124**, 189–199 (2019).
8. D. R. Piperno, *Phytoliths: a comprehensive guide for archaeologists and paleoecologists*. Rowman Altamira (2006).
9. K. Feagri, J. Iversen, *Textbook of Pollen Analysis* (fourth ed.), Wiley, London (1989).
10. S.E. Lowick *et al.*, Luminescence dating of Middle Pleistocene proglacial deposits from northern Switzerland: methodological aspects and stratigraphical conclusions. *Boreas* **44**, 459–482 (2015).
11. A.S. Murray, A.G. Wintle, Dating quartz using an improved single-aliquot regenerative-dose (SAR) protocol. *Radiation Measur.* **32**, 57–73 (2000).
12. Murray, A.S., A.G. Wintle, The single aliquot regenerative dose protocol: potential for improvements in reliability. *Radiation Measur.* **37**, 377–381 (2003).
13. Duller, G.A.T., Distinguishing quartz and feldspar in single grain luminescence measurements. *Radiation Measur.* **37**, 161–165 (2003).
14. F. Preusser, H.U. Kasper, Comparison of dose rate determination using high-resolution gamma spectrometry and inductively coupled plasma-mass spectrometry. *Ancient TL* **19**, 17–21 (2001).
15. J.A. Durcan, G.E. King, G.A.T. Duller, DRAC: Dose Rate and Age Calculator for trapped charge dating. *Quatern. Geochronol.* **28**, 54–61 (2015).
16. S. Kreuzer, C. Schmidt, M. Fuchs, M. Dietze, Introducing an R package for luminescence dating analysis. *Ancient TL* **30**, 1–8 (2012).
17. R.F. Galbraith *et al.*, Optical dating of single and multiple grains of quartz from Jinmium rock shelter, northern Australia: part i, experimental design and statistical models. *Archaeometry* **2**, 339–364 (1999).
18. J. Fietzke *et al.*, Determination of uranium isotope ratios by multi-static MIC-ICP-MS: Method and implementation for precise U- and Th-series isotope measurements. *J. Anal. At. Spectrom.* **20**, 395–401 (2005).
19. C.D. Woodroffe *et al.*, Stratigraphy and chronology of late Pleistocene reefs in the Southern Cook Islands, South Pacific. *Quat. Res.* **35**, 246–263 (1991).
20. P. Vermeesch, IsoplotR: a free and open toolbox for geochronology. *Geosci. Frontiers* **9**, 1479–1493 (2018).
21. C. Paton *et al.*, Lolite: Freeware for the visualisation and processing of mass spectrometric data. *J. Analyt. Atomic Spectrom.* **26**, 2508–2518 (2011).
22. C. Carcaillet, B. Talon, Aspects taphonomiques de la stratigraphie et de la datation de charbons de bois dans les sols : exemple de quelques sols des Alpes. *Géogr. Phys. Quatern.* **50**, 233–244 (1996).
23. M.B. Schiffer, Radiocarbon dating and the “old wood” problem: the case of the Hohokam chronology. *J. Archaeol. Sci.* **13**, 13–30 (1986).
24. M. Molnar *et al.*, Status Report of the New AMS 14C Sample Preparation Lab of the Hertelendi Laboratory of Environmental Studies (Debrecen, Hungary). *Radiocarbon* **55**, 665–676 (2013).
25. C. Bronk Ramsey, OxCal v. 4.4.4. (2021) [<https://c14.arch.ox.ac.uk/oxcal.html>]
26. P. Reimer *et al.*, The IntCal20 Northern Hemisphere radiocarbon age calibration curve (0–55 cal kBP). *Radiocarbon* **62**, 725–757 (2020).
27. A.G. Wintle, Luminescence dating: where it has been and where it is going. *Boreas* **37**, 471–482 (2008).
28. N. Sariaslan, M.R. Langer, Atypical, high-diversity assemblages of foraminifera in a mangrove estuary in northern Brazil. *Biogeosci.* **18**, 1–18 (2021).
29. A.C.S. Almeida, F.B.C. Souza, L.M. Vieira, Malacostegine bryozoans (Bryozoa: Cheilostomata) from Bahia State, northeast Brazil: taxonomy and non-indigenous species. *Marine Biodiv.* **48**, 1463–1488 (2017).
30. L.M. Vieira, A.E. Migotto, J.E. Winston, Synopsis and annotated checklist of Recent marine Bryozoa from Brazil. *Zootaxa* **1810**, 1–39 (2008).
31. D.J. Hughes, J.B.C. Jackson, Do constant environments promote complexity of form?: The distribution of bryozoan polymorphism as a test of hypotheses. *Evolution* **44**, 889–905 (1990).
32. T. Van der Hammen, A palynological study on the Quaternary of British Guiana. *Leidse Geol. Meded.* **29**: 125–180 (1963).
33. D. R. Piperno, *Phytoliths: a comprehensive guide for archaeologists and paleoecologists*, (Rowman Altamira, 2006).
34. C. Crifò, C. A. Strömberg, Small-scale spatial resolution of the soil phytolith record in a rainforest and a dry forest in Costa Rica: applications to the deep-time fossil phytolith record. *Palaeogeogr., Palaeoclimatol., Palaeoecol.* **537**, 109107 (2020).

35. J. Iriarte *et al.*, Late Holocene Neotropical agricultural landscapes: phytolith and stable carbon isotope analysis of raised fields from French Guianan coastal savannahs. *J. Archaeol. Sci.* **37**, 2984–2994 (2010).
36. J. Iriarte *et al.*, Fire-free land use in pre-1492 Amazonian savannas. *Proc. Natl. Acad. Sci. U.S.A.* **109**, 6473–6478 (2012).
37. Durand, J. Les éléments principaux de la faune et leurs relations avec le fond, *Cahiers de l'ORSTOM* **3**, 1–93 (1959).
38. Giachini Tosetto, E. *et al.*, The Amazon River plume, a barrier to animal dispersal in the Western Tropical Atlantic. *Scientific Reports* **12**, 537 (2022).
39. Massemin, D., D. Lamy, J.-P. Pointier, O. Gargominy, Coquillages et escargots de Guyane. *Publications Scientifiques du Muséum, MNHN, Paris* (2009).